Next, we compare the running time of the two methods. Since both methods need the pre-calculation of $A^T A$ and $A^T \Phi$, we set the starting point at the time when $A^T A$ and $A^T \Phi$ were just obtained. Then, the running time of the Newton method for three different phantom setups was 166.62s, 189.32s and 180.09s, respectively. And the running time of the proposed method was 1.16s, 2.11s and 4.46s, respectively. The proposed method is much more efficient.

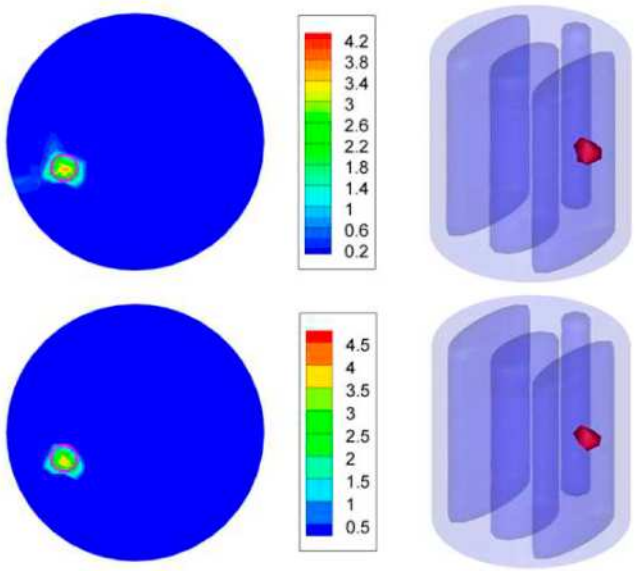

Fig. 3. Reconstruction results from the Newton method (first row) and the iterated shrinkage based method (second row) for 1 spherical fluorescent source and 15 measurement data sets. These results are presented in the form of slice images in z = 0 plane (left column) and iso-surfaces for 30% of the maximum value (right column). The small circles in the slice images denote the real positions of the fluorescent sources.

Table 2. Quantitative comparisons between the results from the Newton method with Tikhonov regularization (Newton-L2) and the iterated shrinkage based method with L1 regularization (IS-L1) for 15 measurement sets

Phantom setup	Source No.	Location error (*mm*) (Newton-L2)	Location error (*mm*) (IS-L1)	Relative intensity error (Newton-L2)	Relative intensity error (IS-L1)
1 source	S	0.39	0.39	44.5%	38.2%
2 sources	S1	0.39	0.39	70.0%	45.3%
	S2	0.85	0.85	75.9%	66.4%
3 sources	S1	0.25	0.25	74.4%	33.0%
	S2	0.97	0.97	75.3%	63.4%
	S3	0.73	0.73	71.8%	63.8%

#122686 - $15.00 USD Received 13 Jan 2010; revised 25 Mar 2010; accepted 1 Apr 2010; published 9 Apr 2010

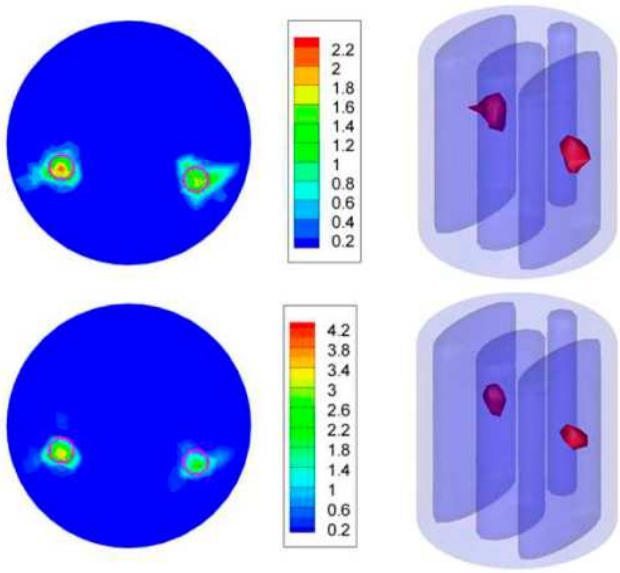

Fig. 4. Reconstruction results from the Newton method (first row) and the iterated shrinkage based method (second row) for 2 spherical fluorescent sources and 15 measurement data sets. These results are presented in the form of slice images in z = 0 plane (left column) and iso-surfaces for 30% of the maximum value (right column). The small circles in the slice images denote the real positions of the fluorescent sources.

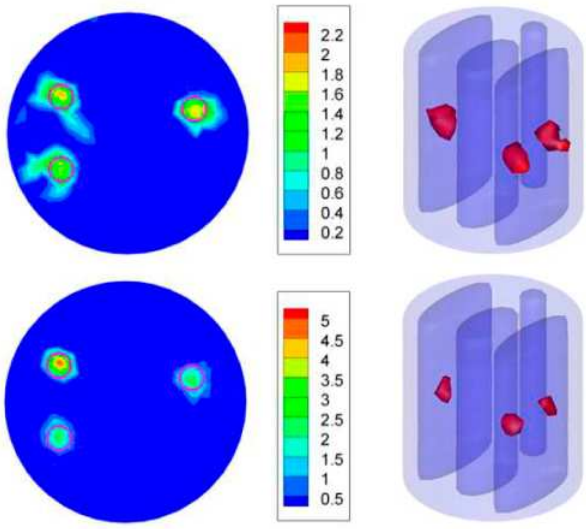

Fig. 5. Reconstruction results from the Newton method (first row) and the iterated shrinkage based method (second row) for 3 spherical fluorescent sources and 15 measurement data sets. These results are presented in the form of slice images in z = 0 plane (left column) and iso-surfaces for 30% of the maximum value (right column). The small circles in the slice images denote the real positions of the fluorescent sources.

In the second set of experiments, we reduced the amount of measurement data to simulate a much worse case. This is possible when long-time measurement is not appropriate or feasible. For instance, when imaging small animals like mice, the artifacts caused by movements must be taken into consideration. Besides, long-time measurement can cause the bleaching effect of the fluorescent probe, which may influence the reconstructed results. One way to resolve these problems is to reduce the number of fluorescence measurements. This

#122686 - $15.00 USD Received 13 Jan 2010; revised 25 Mar 2010; accepted 1 Apr 2010; published 9 Apr 2010

requires that we should be able to reconstruct the fluorescent sources from very limited data. It has been shown for bioluminescence tomography that, by using sparsity constraint, satisfactory results can still be achievable even with very limited imaging data [8]. Here, we only retained the measurement data sets generated by excitation point source 1, 6 and 11. Figures 6, 7 and 8 show the reconstruction results in this case. From these figures we can see that, when the measurement data is very limited and multiple fluorescent sources exist, the proposed method can obtain much better results compared to the Newton method with Tikhonov regularization. This demonstrates the applicability of the proposed method under more ill-posed conditions. Quantitative comparisons are presented in Table 3. For the Newton method, the reconstruction errors for source S1 and S2 in the third phantom setup are not presented, because the two sources cannot be separated in the result. The running time of the Newton method for three different phantom setups was 183.98s, 173.91s and 168.02s, respectively. And the running time of the proposed method was 1.84s, 2.97s and 2.42s, respectively.

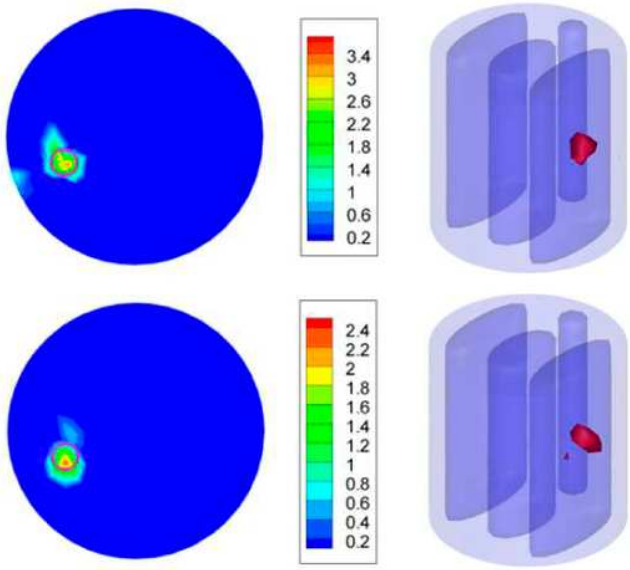

Fig. 6. Reconstruction results from the Newton method (first row) and the iterated shrinkage based method (second row) for 1 spherical fluorescent source and 3 measurement data sets. These results are presented in the form of slice images in z = 0 plane (left column) and iso-surfaces for 30% of the maximum value (right column). The small circles in the slice images denote the real positions of the fluorescent sources.

Table 3. Quantitative comparisons between the results from the Newton method with Tikhonov regularization (Newton-L2) and the iterated shrinkage based method with L1 regularization (IS-L1) for 3 measurement sets

Phantom setup	Source No.	Location error (*mm*) (Newton-L2)	Location error (*mm*) (IS-L1)	Relative intensity error (Newton-L2)	Relative intensity error (IS-L1)
1 source	S	0.39	0.39	53.5%	68.9%
2 sources	S1	2.00	1.62	91.4%	71.4%
	S2	0.85	0.85	84.4%	64.0%
3 sources	S1	——	0.25	——	29.3%
	S2	——	0.97	——	56.3%
	S3	0.73	0.73	87.0%	60.2%

#122686 - $15.00 USD Received 13 Jan 2010; revised 25 Mar 2010; accepted 1 Apr 2010; published 9 Apr 2010

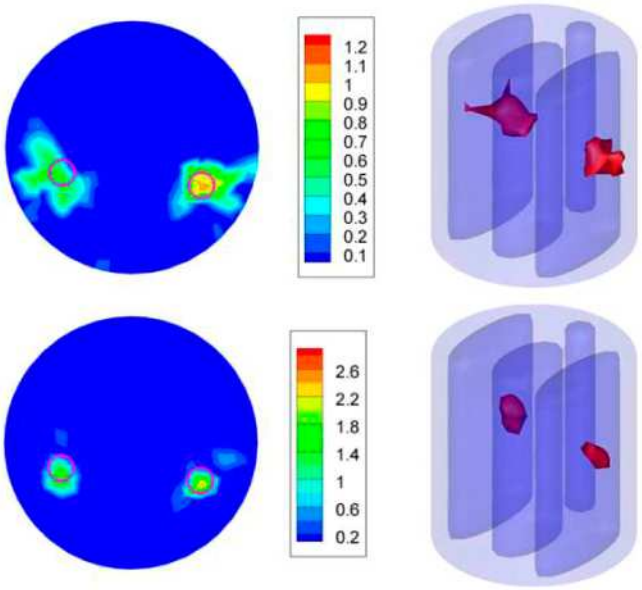

Fig. 7. Reconstruction results from the Newton method (first row) and the iterated shrinkage based method (second row) for 2 spherical fluorescent sources and 3 measurement data sets. These results are presented in the form of slice images in z = 0 plane (left column) and iso-surfaces for 30% of the maximum value (right column). The small circles in the slice images denote the real positions of the fluorescent sources.

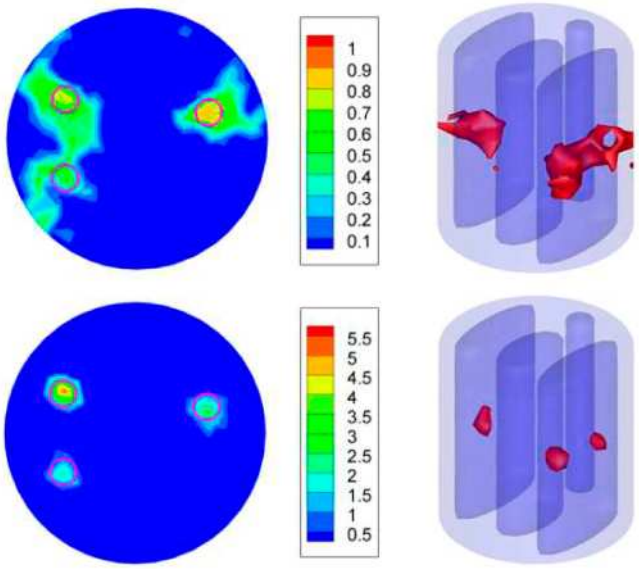

Fig. 8. Reconstruction results from the Newton method (first row) and the iterated shrinkage based method (second row) for 3 spherical fluorescent sources and 3 measurement data sets. These results are presented in the form of slice images in z = 0 plane (left column) and iso-surfaces for 30% of the maximum value (right column). The small circles in the slice images denote the real positions of the fluorescent sources.

#122686 - $15.00 USD Received 13 Jan 2010; revised 25 Mar 2010; accepted 1 Apr 2010; published 9 Apr 2010

3.2 Physical experiments

In this subsection, physical experiments were conducted to further test the proposed algorithm. Figure 9 illustrates the experimental setup. Excitation illumination was provided by a 671nm CW laser and the power was set to 20mW. The spot diameter of the laser beam was approximately 1mm. The fluorescence measurements were implemented in transillumination mode. A 10nm band-pass filter centered at 700nm was used to allow light transmission at the emission wave-length. The optical density of the filter at the excitation wave-length was larger than 5. Fluorescence was captured by a CCD camera (Princeton Instruments VersArray 1300B, Roper Scientific, Trenton, NJ) which was cooled to −110°C.

To reconstruct the sources, the pixels of the measured fluorescence image should firstly be converted into the corresponding photon flux densities. Then, the calibrated image needs to be back-projected onto the surface of the phantom. Errors can be introduced during the mapping procedure. To avoid this problem and to test only the performance of the proposed reconstruction method, a cubic phantom was utilized in this experiment, and the back-projection was reduced to a point-to-point mapping. Figure 10(a) shows the phantom we used. The side length is 20mm. The phantom is made from polyoxymethylene, and the optical parameters for both excitation and emission wave-lengths, which are presented in Table 4, were determined by diffuse optical tomography. The sparsity-promoting characteristic of the proposed method can be better demonstrated when more than one source exists, which can be seen from our simulation results. Therefore, in this experiment, two small holes of 1.25mm in radius were drilled to allow two fluorescent sources. 2000nM Cy5.5 solution was used as the fluorescent source. The height of the two cylindrical sources was 2mm, and the centers were at (−3.75mm, 3.75mm, 1mm) and (3.75mm, −3.75mm, 1mm) respectively, which is illustrated in Fig. 10(b). To simulate a badly ill-posed situation, fluorescence was excited by point sources from only 4 different locations in $z = 0$ plane, which is illustrated in Fig. 10(c). The phantom was placed on a rotational stage, which was controlled by computer, to allow measurements from four sides.

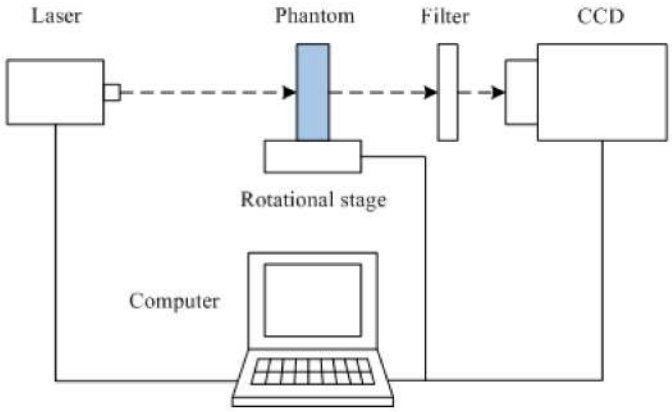

Fig. 9. The sketch of the experimental setup.

Table 4. Optical parameters of the cubic phantom

Wave-length (*nm*)	$\mu_a(mm^{-1})$	$\mu_s'(mm^{-1})$
671	0.00029	1.08
700	0.00051	1.11

#122686 - $15.00 USD Received 13 Jan 2010; revised 25 Mar 2010; accepted 1 Apr 2010; published 9 Apr 2010

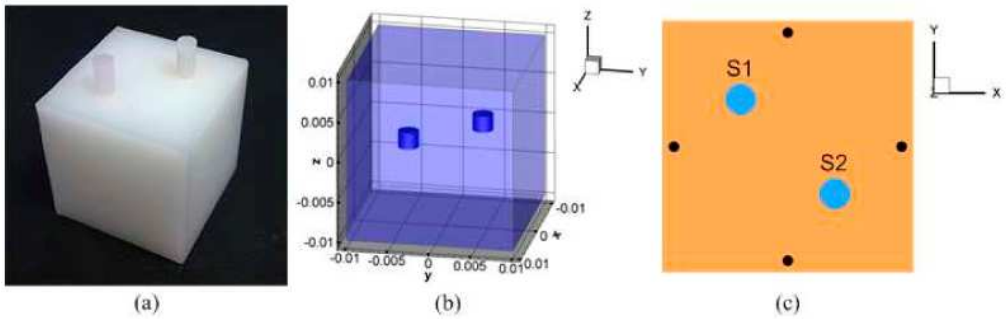

Fig. 10. The homogeneous cubic phantom with 2 cylindrical fluorescent sources. (a) is the photograph of the phantom. (b) is the 3D view of the phantom and the sources. (c) is the slice image of the phantom in z = 0 plane. The black dots in (c) represent the excitation point source locations.

In this experiment, the cubic phantom was discretized with tetrahedrons. For the forward problem, a fine mesh with about 21000 DOFs was adopted. And a coarse mesh with 2705 DOFs was used for the inverse problem. Figure 11 shows the reconstruction results which are presented in the form of slice images in $z = 1mm$ plane and iso-surfaces for 30% of the maximum value. From Fig. 11 we can clearly see that, due to the badly ill-posed situation and the over-smooth effect of Tikhonov regularization, the reconstructed fluorescent sources from the Newton method are spread within the entire domain, which makes result totally meaningless. The location errors are not presented for the Newton method, because the source locations cannot be identified from the result. On the contrary, the proposed method with L1 regularization can preserve the sparsity of the fluorescent sources very well, though some artifacts exist near the center. The location errors for the fluorescent sources S1 and S2 were 1.21mm and 0.82mm, respectively. The running time of the Newton method and the proposed method was 135.91 seconds and 2.56 seconds, respectively.

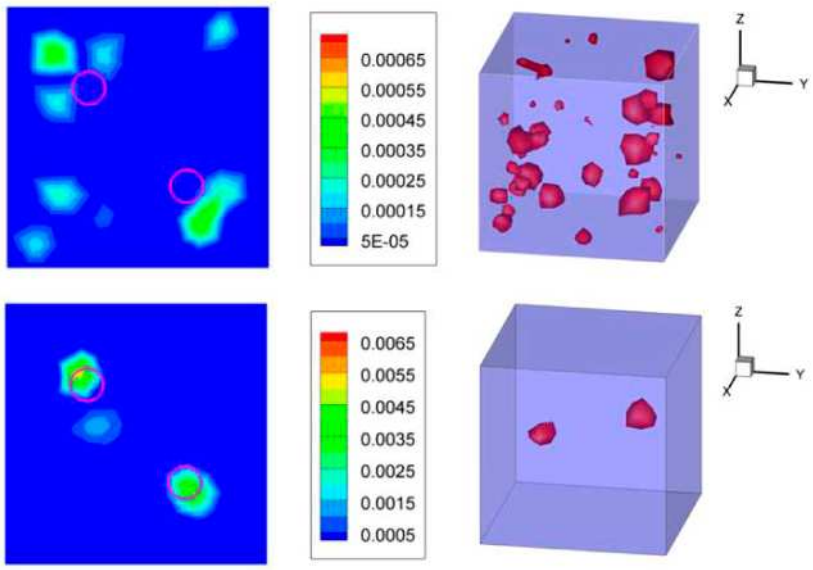

Fig. 11. Reconstruction results of the cubic phantom from the Newton method (first row) and the iterated shrinkage based method (second row) using 4 measurement data sets. These results are presented in the form of slice images in z = 1mm plane (left column) and iso-surfaces for 30% of the maximum value (right column). The small circles in the slice images denote the real positions of the fluorescent sources.

#122686 - $15.00 USD Received 13 Jan 2010; revised 25 Mar 2010; accepted 1 Apr 2010; published 9 Apr 2010

4. Conclusion

In this paper, an iterated shrinkage based reconstruction algorithm is proposed. By integrating an additional surrogate function, the original high dimensional optimization problem can be decoupled into a set of one dimensional ones that can be solved easily. This also enables us to incorporate sparsity regularization in a graceful way. Two reconstruction strategies are provided for different situations together with their complexity analysis. Besides, we explain that due to the sparsity characteristic of the fluorescent sources, the efficiency of the algorithm can be greatly improved, which leads to a fast reconstruction method. Simulation verifications show that the proposed method outperforms the traditional bound-constrained Newton method with Tikhonov regularization in two ways. First, due to the sparsity constraint of our method, obvious improvements can be seen from these reconstruction results. Second, our method is much faster than the Newton method when the fluorescent sources are sparse. This is important if we want to transfer FMT into practical use. We also test our method under a more ill-posed condition and satisfactory results can still be achievable. Reconstruction of experimental data further demonstrates the performance of the proposed method.

For FMT reconstruction, the choice of the regularization parameter will have a significant impact on the results. A large parameter value can make the reconstructed solution deviate from the real distribution, while a small value will have little contribution to the regularization of the problem. Finding the optimal or near-optimal regularization parameter automatically still remains a challenging task. Generally speaking, two strategies can be used: determine the parameter in advance or update it heuristically. This will be our future research.

Another important issue lies in the accuracy of the photon propagation model itself. The diffuse equation has been extensively utilized to describe light transport in biological tissue, yet it is not applicable in certain regions, such as void or more absorptive regions. Several improved models, e.g. higher order approximation to radiative transfer equation, have been proposed to resolve the problem, though more computations are typically needed and the physical meanings are not such explicit. Since FMT reconstruction is a linear inverse problem in nature, the proposed reconstruction algorithm can potentially be utilized in these improved models.

In conclusion, we have developed a fast reconstruction algorithm with sparsity constraint for FMT. Numerical simulations and physical experiments show the merits of our method compared to the Newton method with Tikhonov regularization. *In vivo* mouse studies using the proposed method will be reported in the future.

Acknowledgments

This paper is supported by the Project for the National Basic Research Program of China (973) under Grant No.2006CB705700, Changjiang Scholars and Innovative Research Team in University (PCSIRT) under Grant No.IRT0645, CAS Hundred Talents Program, CAS scientific research equipment develop program under Grant No. YZ200766, the Knowledge Innovation Project of the Chinese Academy of Sciences under Grant No. KGCX2-YW-129, KSCX2-YW-R-262, the National Natural Science Foundation of China under Grant No. 30672690, 30600151, 60532050, 60621001, 30873462, 60910006, 30970769, 30970771, Beijing Natural Science Fund under Grant No.4071003, Science and Technology Key Project of Beijing Municipal Education Commission under Grant No.KZ200910005005.

#122686 - $15.00 USD Received 13 Jan 2010; revised 25 Mar 2010; accepted 1 Apr 2010; published 9 Apr 2010